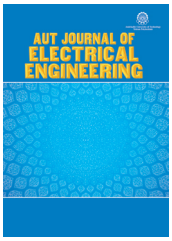

AUT Journal of Electrical Engineering

AUT J. Elec. Eng., 49(2)(2017)109-122
DOI: 10.22060/eej.2017.13219.5142

A Review of Application of Signal Processing Techniques for Fault Diagnosis of Induction Motors – Part I

J. Faiz[1*], A. M. Takbash[2], E. Mazaheri-Tehrani[1]

[1] School of Electrical and Computer Engineering, College of Engineering, University of Tehran, Iran
[2] Department of Electrical and Computer Engineering, Concordia University, Montreal, Canada.

ABSTRACT: The use of efficient signal processing tools (SPTs) to extract proper indices for fault detection in induction motors (IMs) is the essential part of any fault recognition procedure. In the first part of the present paper, we focus on Fourier-based techniques, including fast Fourier transform and short time Fourier transform. In this paper, all utilized SPTs which have been employed for fault detection in IMs are analyzed in detail. Then, their competency and their drawbacks to extract indices in transient and steady state modes are criticized from different aspects. Different kinds of faults, namely, eccentricity, broken bar, and bearing faults as the major internal faults in IMs, are investigated.

Review History:
Received: 31 July 2017
Revised: 27 August 2017
Accepted: 27 August 2017
Available Online: 23 October 2017

Keywords:
Fault diagnosis
induction motors
signal processing
Fourier transform
eccentricity fault
broken bars fault
bearing fault

1- Introduction

Ever-increasing application of induction motors (IMs) in different industries and importance of eliminating its uninterrupted operation in production lines make it necessary to diagnose internal faults in these motors quickly and precisely. Electrical, mechanical, magnetic, and thermal stresses caused by improper operation of the machines are the main reasons for the occurrence of these internal faults.

With the development of powerful microprocessors, signal processing tools (SPTs) became an integral part of every fault diagnosis system and contributed to the more reliable condition monitoring schemes. A plethora of SPTs has been proposed in the literature for diagnostic purposes. Generally, SPTs can be categorized into two main branches, namely stationary and non-stationary. When a machine pursues a stable regime, called stationary conditions, Fourier transform can be used as a powerful tool for the decomposition of faulty signals and tracking fault components. On the other hand, under non-stationary conditions, in which most of the machine signals are not periodic, time-frequency methods should be used for this purpose in order to track fault harmonics over the time.

In this paper, as the first part of a review, Fourier transform and its extended version for non-stationary conditions, called short-time Fourier transform, are investigated. The application of these tools for the diagnosis of different internal faults of IMs is studied. Furthermore, the impact of external factors such as load variations and drive systems are studied. A similar approach will be followed for the other types of SPTs in the second part.

The corresponding author; Email: jfaiz@ut.ac.ir

2- Internal Faults in Induction Machines

The internal faults in induction motors consist of electrical and mechanical faults. Electrical faults occur in the stator and rotor. Stator faults include a short circuit in stator windings. This short circuit may happen between two turns, two windings, one phase of winding and earth or two phases of one winding. It is noted that one fault may result in other faults. Fig. 1 shows the relationship between different stator internal faults. Diagnosing and predicting the stator faults are simpler than other internal faults of the motor. The reasons are: 1) these faults are strong at initial stages and exhibit more clear effects and signs, and 2) the stator is more accessible compared to other parts of the machine. Electrical faults of the squirrel-cage rotor of induction motor consist of bars and end-rings breakage, which are about 10% of the internal faults of squirrel-cage induction machine [1-2]. The reasons for such faults are as follows:

1. thermal stresses due to over-load and asymmetrical dissipation of heat and generation of the hot spot,
2. magnetic stresses arising from electromagnetic forces,
3. stresses due to assembling process,
4. stresses due to centrifugal forces arising from shaft torque,
5. mechanical stresses due to the mechanical fatigue of different parts, bearing damage, etc.

Some impacts of the broken bars on induction motor are as follows:

1. the presence of the 3rd harmonic magnetic flux density in the air gap [3,4],
2. the increasing of core losses and total losses in faulty machine [3–5],
3. asymmetrical vector diagram of rotor current, this should be fully symmetrical in a healthy motor [3],
4. the reduction of leakage reactance and effective resistance of the bars adjacent to the broken bar [3].

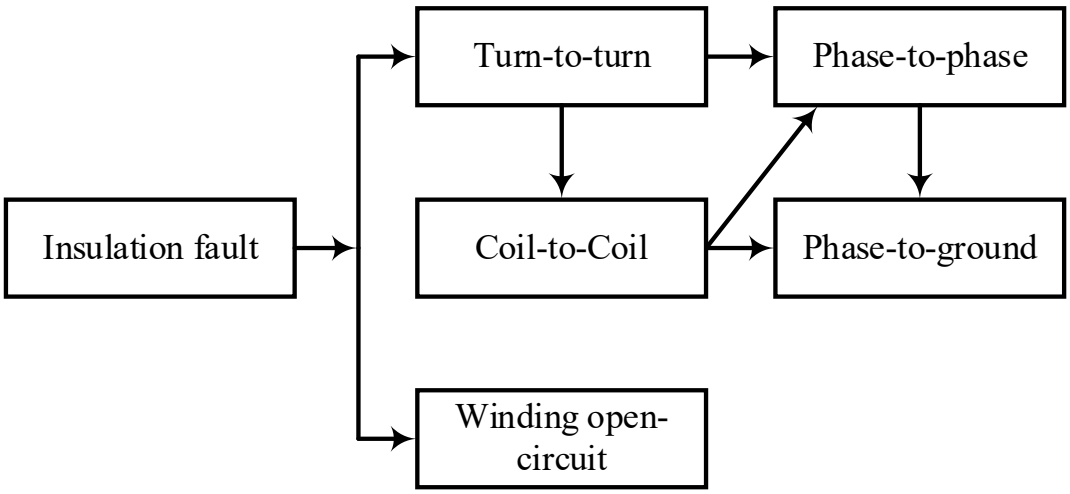

Fig. 1. Relation between various internal faults of stator [1]

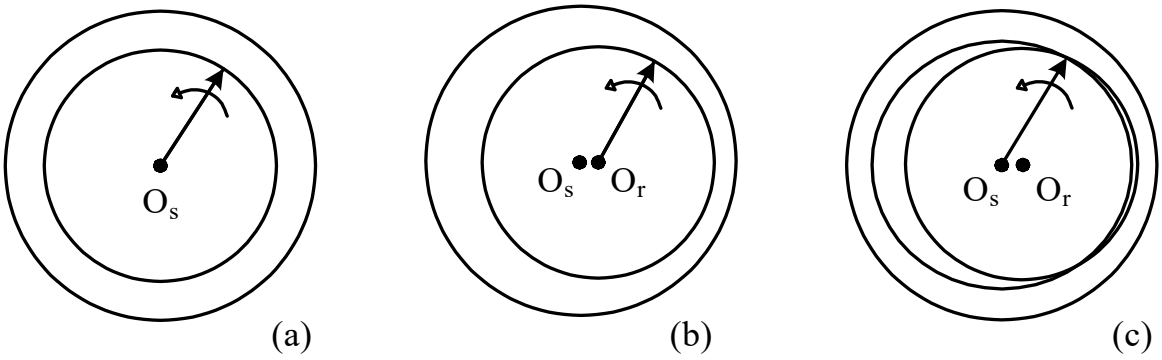

Fig. 2. Different types of eccentricity faults, (a) Healthy motor, (b) Static eccentricity, (c) Dynamic eccentricity.

Broken bars and end ring faults have been studied more than other types of internal faults in the induction motor. In addition to these electrical faults in the squirrel-cage rotor, some faults similar to the stator winding may occur in the squirrel-cage rotor. The mechanical faults, including bearing and eccentricity faults, are those faults that occur in the mechanical parts of the motors.. Statistics show that 80% of faults in motors are because of the eccentricity [1-6]. This fault may occur due to the stator oval structure, assembling problems of motor [7-8], operation of the motor at critical speed [9], and mechanical resonance at the critical load [8]. There is static, dynamic, and mixed eccentricity as shown in Fig. 2. Being incautious to this fault and neglecting its on-time diagnosis can seriously cause damages to the motor, that they are the rubbing and the abrasion of the rotor to stator. That is why great attention has been paid to this fault in the last two decades [7, 10]. There is an inherent static eccentricity in the motor. This causes a stable asymmetry in the magnetic pulling of the motor, bending the shaft, weakening the bearings, and finally leading to a dynamic eccentricity [7, 11]. Motors may also have an inherent dynamic eccentricity [10]. Eccentricity creates a magnetic pull that leads to the separation of the stator and rotor axes. This magnetic pull is constant and unidirectional for static eccentricity and rotates with a field for the dynamic eccentricity. The magnetic force leads to the stress on the stator windings [9]. Since eccentricity fault and load current effects on the current spectrum are similar, it is difficult to diagnose this fault [12]. To detect this fault, variations in the frequency spectrum of different signals, including current waveforms, are used.

One of the mechanical faults of the motor which involves 41% of the internal faults of the induction motor is the bearing fault [13]. This fault does not generate an instantaneous problem in the motor and gradually affects it. Also, this fault increases friction losses and decreases the efficiency [14]. Fig. 3 shows the structure of the healthy bearing. The bearing fault may occur by the current passing through the bearing and this causes wrinkle of the external body of the bearing and rises noise and vibration levels [15]. The bearing faults can be categorized into two general groups, as shown in Fig. 4 [13] or four groups [14, 16, 17]. The bearing fault generates two types of linear and radial movements of stator and rotor which can be used for the detection of this fault. The important point about internal faults of the motor is that the most internal faults finally lead to mechanical faults [1]. Fig. 5 shows a general view of different faults in an induction motor [18]. The faulty motor is studied using experimental or modeling and simulation methods. Magnetic equivalent circuit (MEC) is one of the motor modeling techniques in which MEC is applied to all components of the motor. This model shows the passing flux path. In this model, a numerical magnetic potential is defined for every node. The current passing each permeance indicates the flux of that element. Fig. 6 shows a portion of a typical 2-D MEC for an induction motor[1].

Another method is finite difference (FD) method in which the resulting differential equations are transformed into the difference ones. One of the major methods in modeling a faulty motor is the winding function (WF) [19]. This method

calculates the inductances of the motor, taking into account the spatial harmonics due to the winding distribution. Then, using dynamic equations, the currents can be calculated. Given the current and inductance, electromagnetic torque is computed and replaced in the mechanical equations of the motor. Two major assumptions in the application of this method include neglecting mmf drop of the iron and radial air gap field [12]. The drawbacks of WFM are that this model cannot model saturation versus time averaging permeance, slot effect upon air gap permeance; therefore, FEM is preferable. Fig. 7 shows the rotor cross-section. FEM gives the magnetic field pattern of the motor using its geometry and magnetic parameters. Other parameters of the magnetic field such as air gap flux density can be calculated with the knowledge of the magnetic field distribution. FEM is more precise compared to other methods but it is a time-consuming technique [1].

Following the analysis of faulty motor by test or modeling, a proper signal must be selected. The signals used in the fault diagnosis process, consist of mechanical and electrical signals. Mechanical signals are composed of torque, speed, motor body vibration and temperature. Electrical signals consist of stator voltage, stator current, and air gap flux density. For three reasons, the stator current signal is a suitable signal for the fault diagnosis. The first reason is the unique effect of the motor internal fault on this signal. The second is that there is no need to have a sensor for monitoring this signal. The third reason is that this method is economical. After testing or modeling the motor and selecting a proper signal, it must be processed and the effect of the proposed fault upon the signal is determined. This is the aim of application of different processors. The signal processing methods are based on the mathematical transformations. Fourier transform is a well-known and powerful tool for the condition-monitoring of electrical machines, and an enormous number of researches are devoted to it. However, these conventional methods are only applicable to steady-state signals of the machines with a stable regime which is not common in the industry. In addition, other inherent transient signals of the machines such as start-up currents and switch-off terminal voltages which may have useful information for the fault detection, cannot be investigated with classical tools. To solve this problem and reveal the underlying dynamics that correspond to the signal, recently modern signal processing tools such as time-frequency transforms are required to deal with these non-stationary signals. Wavelet transform, Hilbert-Huang transform and multiple signal classification (Music) are of these methods which are used for this purpose. Recently, intelligent methods such as Genetic algorithm, Fuzzy logic, and Artificial Neural Networks have been applied to make the fault diagnosis decision more efficient [16, 20, 21]. It is impossible and unscientific to decisively determine one of the above-mentioned processing methods as the best method for all signals, different internal faults, and load conditions. With considering the fault type, the load conditions, and the proposed processor characteristics, a particular processor will be selected for each case. To choose an appropriate processor, different faults and operating conditions such as the load conditions are considered. Since harmonics caused by motor internal fault depend on the load condition and level, more emphasis is put on the load. Note that the above-mentioned harmonics are close to the fundamental harmonic under the light load; hence, the fault diagnosis will be difficult.

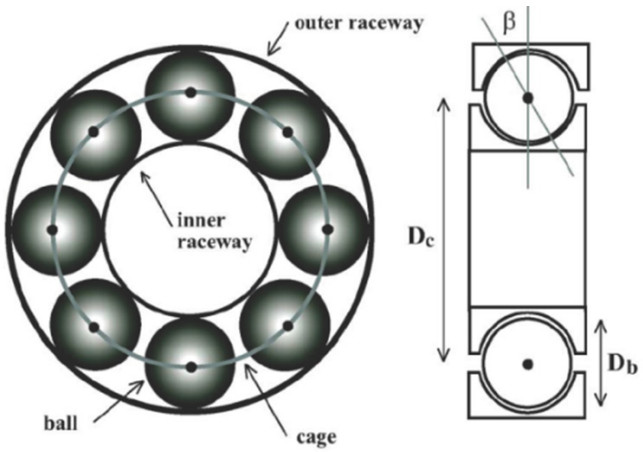

Fig. 3. Structure of healthy bearing [14]

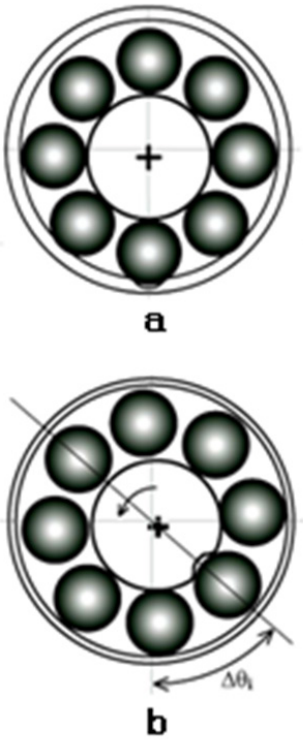

Fig. 4. Axial and radial movement caused by bearing fault [13]

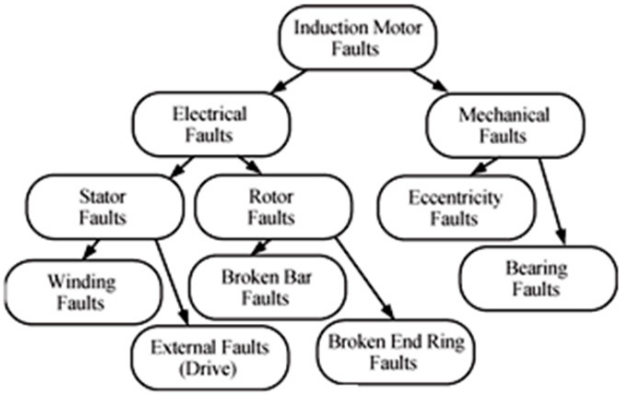

Fig. 5. General view of different faults in induction motors [18]

3- Fourier Transform

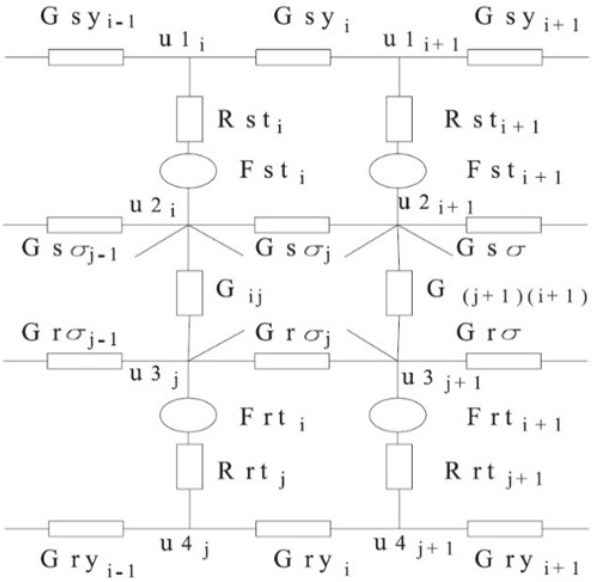

Fig. 6. A typical 2D MEC of induction motor rotor [1]

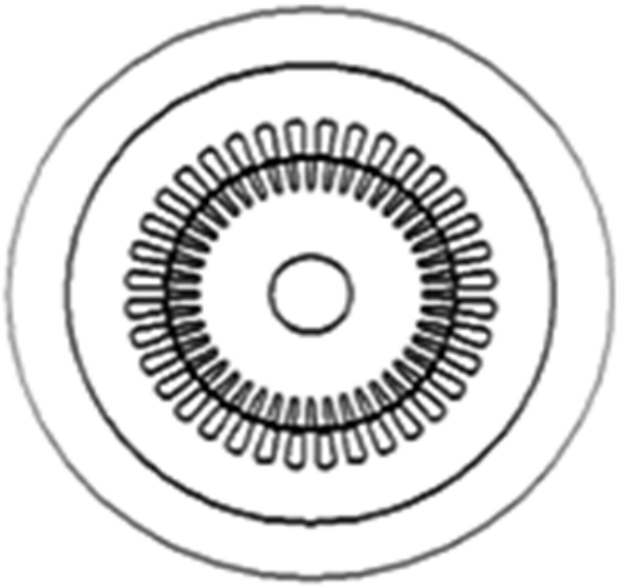

Fig. 7. Rotor cross-section [1]

Spectral analysis of the faulty machines is a common tool for fault diagnosis. Fourier transform expresses signal as a sum of sinusoidal functions. This tool expresses a time-domain signal in the frequency-domain using a linear transform. The aim of using this transform is to determine the frequency components arising from the faults which are not known a priori. The discrete version of this transform for the analysis of the digital signals called discrete Fourier transform (DFT) is time consuming with computational complexity of $O(N^2)$ for a signal with the length of N. Therefore, usually DFT is implemented by the fast Fourier transform (FFT) in order to increase the computation speed and, in this case, computational complexity will be reduced to O(NlogN). To obtain a high-frequency resolution and avoid spectral leakage, it is necessary to calculate the Fourier transform of signals read over a long time. In fault diagnosis applications, capturing signals over a long period of time will increase the risk of the influence of load and power supply on the signal. Also, it is observed that rotor core anisotropy created during the rolling process will cause a false alarm in condition-monitoring systems and sensorless control drives. A comprehensive study of the influence of anisotropy on the rotor fault components can be found in [22]. In addition, these transforms are not applicable to cases in which signals are non-stationary. Therefore, an extended version of Fourier transform for non-stationary conditions, called Short Time Fourier Transform (STFT), is proposed. The major issue in this method is the determination of the length and the type of the window in which signals are assumed to be stationary and Fourier transform is applicable for. STFT is a fixed resolution method and the length of the window should be adjusted appropriately depending on the application [19].

3- 1- Rotor Bars and End Ring Breakage

For the rotor bars and end ring breakage fault diagnosis in the induction motor, Fourier-based techniques are used often used, and the frequency spectra of torque, speed, instantaneous power, body vibration, zero sequence currents, and stator current signals are obtained. Torque signal has been employed as a reference for the fault diagnosis in [4, 21, 23]. The harmonics 2sfs are produced in the torque frequency spectrum used for the fault detection. Fig. 8 shows the frequency spectrum of a typical induction motor torque under the bars fault [24]. The influence of the location of the broken bar on the amplitude of the torque harmonics has been pointed out in [25]. Table 1 presents this effect.

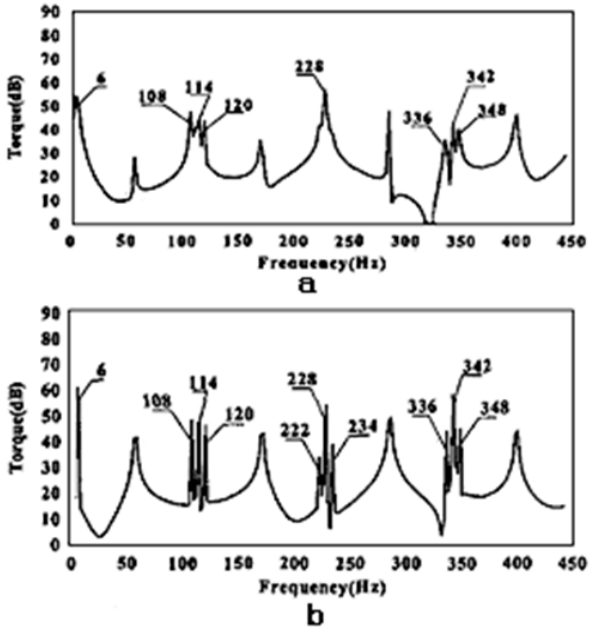

Fig. 8. Torque frequency spectrum: (a) healthy motor, (b) broken-bars motor [24].

The amplitude of torque harmonics is increased by more concentration of the broken bars. Some references, e.g. [24], use the speed signal for the fault diagnosis, and, here, harmonics 2sfs of the frequency spectrum are again proposed. Fig. 9 exhibits the frequency spectrum of speed signal and its variations due to the broken bars [4]. Torque and speed signals depend on the external factors such as load. This fact makes fault diagnosis hard.

In most cases, these signals are considered complementary and confirmatory to the other methods. The influence of the load is arisen from torque fluctuations and appears in the form of harmonics in the frequency spectrum of line current whose equivalence can be determined in speed or torque spectrum [26]. Also, the procedure for acquiring these signals is an important issue because using sensors and other devices affect the accuracy of the operation.

Another signal considered for the fault diagnosis is the case vibration signal. The reason for this vibration is the air gap radial electromagnetic forces. Rotor broken bars cause odd harmonics in the frequency spectrum of the vibration signal. Although sometimes signal with a frequency twice of the supply frequency has been used for the fault diagnosis, this signal is not suitable because it also appears in the frequency spectrum of the vibration signals for a healthy motor [27]. Fig. 10 shows the frequency spectrum of the vibration signal for a healthy motor and a motor with three broken bars at the rated load. The above-mentioned signal depends on the load and its detection requires a sensor [27]. On the other hand, Fourier transform on transient signals, namely speed and vibration, does not yield accurate results.

Pendulum oscillations and increment of load angle ($\Delta\delta$) have been used to detect broken bar [28, 29]. Fig. 11 presents oscillation angle for both healthy and faulty motors [28]. Oscillation of $\Delta\delta$ have been mathematically proposed in [29] with some simplifying assumptions. As seen, broken bars generate 2sfs harmonics in δ spectrum [28].

Instantaneous power signal can also be utilized for the broken bars and end rings fault diagnosis. Advantages of using instantaneous power spectrum are as it follows [30].

1. A large number of low-frequency harmonics exist.
2. Filtering DC component of power is simpler than deleting a current fundamental component, particularly over the low slip.
3. There are only one DC component and one 2fs component in the instantaneous power spectrum of the healthy motor, however, the broken bars fault generates 2ksfs and (2±2ks)fs frequencies [20].
4. The drawback of the application of the instantaneous power spectrum with FFT is its high sensitivity to noise which cannot be eliminated by filtering [26].

In addition to the above-mentioned signals, there are some other signals used for fault detection. The output voltage harmonics of a motor after the power supply interruption can be used to diagnose the fault. The main idea of this method is eliminating the harmonics caused by the voltage supply. Fig. 12 shows the output voltage of the motor after a power supply interruption [31]. However, this signal is a transient signal and FFT application on this signal leads to an inaccurate fault detection. Intelligent algorithms can be used to diagnose the fault through current signal envelope [32]. It is noted that to extract envelope signal particularly in the drive side supply drive, LPF is used to prevent the error caused by drive harmonics. The drawback of this method is that the harmonics of the envelope signal depend on the severity of the rotor bar fault as well as their locations [31]. The current signal has been considered as the most appropriate signal for the internal fault diagnosis. Some references, see e.g. [33], use time spectrum of the line current for fault diagnosis but this fault is often detected through line current harmonics [1–4].

Table 1. Sideband harmonics of torque spectrum for rotor broken bars in different cases [24]

Location of broken bars	Amplitude of harmonics 2sfs
Four broken bars on one pole	-24
Three broken bars on one pole and one broken bar on adjacent pole	-25
Three broken bars on one pole and one broken bar on the opposite pole	-28
Two broken bars on one pole and two broken bars on the adjacent pole	-30
Two broken bars on one pole and two broken bars on two adjacent poles	-33
Two broken bars on one pole and one broken bar on the adjacent and opposite pole	-35
Two broken bars on one pole and two broken bars on opposite pole	-38
One broken bar on each pole	-40
Healthy motor	-59

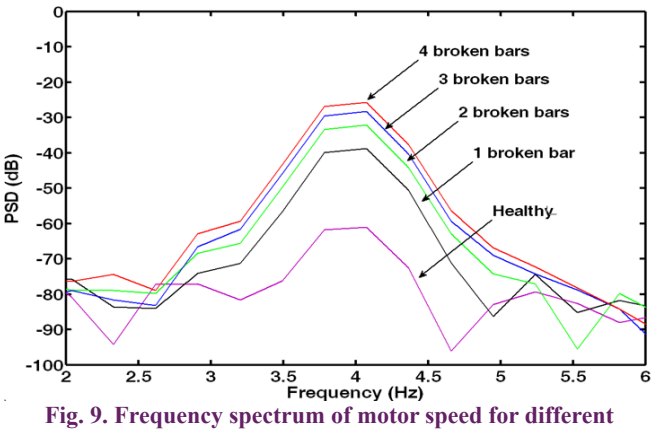

Fig. 9. Frequency spectrum of motor speed for different numbers of rotor broken bars [4].

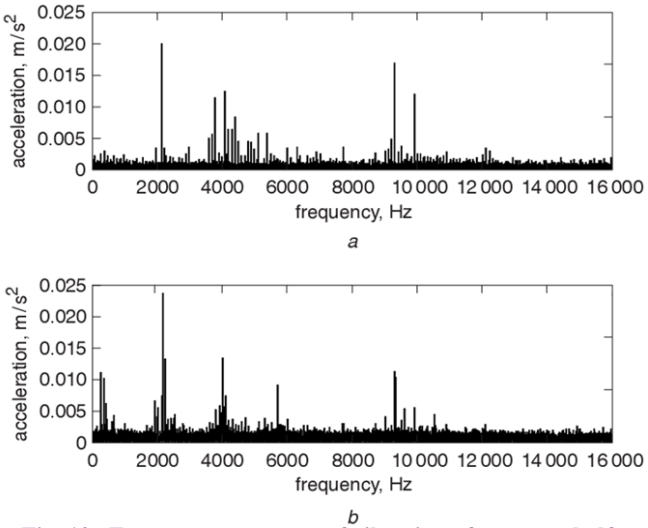

Fig. 10. Frequency spectrum of vibration of motor at half-load: (a). Healthy and (b). Three broken bars motor [27].

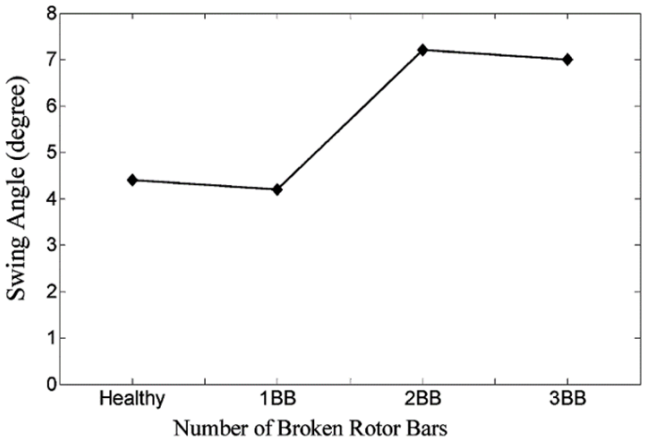

Fig. 11. Variations of motor oscillation angle against numbers of rotor broken bars [28]

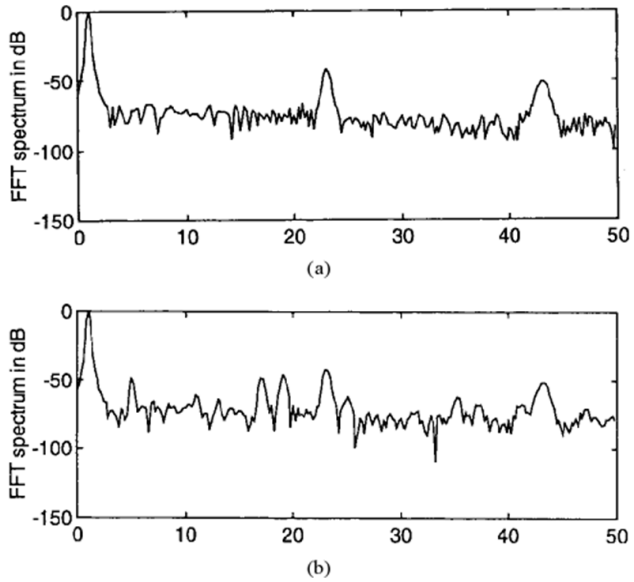

Fig. 12. Frequency spectrum of output voltage after power supply interruption: (a). healthy motor, (b) motor with three broken bars motor [31].

3- 1- 1- Broken Bars and End Ring Fault Diagnosis

The most important harmonics used for the fault diagnosis are (1±2s)fs. The amplitudes of these harmonics are larger than those of other harmonics, and their diagnosis is easier. The amplitude of harmonic (1-2s)fs depends on the rotor broken bars fault and its intensity and harmonic (1+2s)fs is mostly dependent on the speed variations [2]. It is noted that harmonic (1-2s)fs may disappears when broken bars has a 90º phase difference [26]. Also, static eccentricity fault may cause harmonics to be similar to those generated by the broken bars [5]. These harmonics may also be produced by load fluctuations, voltage variations, bearing fault [27], magnetic anisotropy, and misalignment of the shaft and cage [34]. In addition, gearbox application and rotor spider lead to the harmonics similar to those from the broken bar fault [35]. Skewing and non-isolated rotor bars against the core decrease the amplitudes of these harmonics [26]. The fault is diagnosed through stator steady-state current harmonic frequency spectrum using (1±2s)fs harmonics [4, 24, 36, 37]. These harmonics also exist in the frequency spectrum of a healthy motor. However, amplitudes of these sidebands harmonics grows by the broken bars fault. The reason for the rise of the amplitude is the asymmetry of the rotor that is caused from the fault and, consequently, a negative rotating field [36]. Table 2 shows these harmonics before and after the fault [4]. These sideband harmonics exist in a healthy motor and according to the table, the fault in the motor causes large changes in the amplitudes of the harmonics, particularly high sideband harmonics. However, rising the fault intensity produces lower changes in the amplitudes of the sidebands. This reason increases the number of parallel paths of the currents and saturation due to the asymmetry of the currents passing through the bars. Fig. 13 shows the frequency spectrum of the stator current for the broken bars [4]. The discrepancy between the experimental and simulation results comes from neglecting the load effects and inner current of the broken bars. The influence of the bar's inner current in the broken bar fault has been considered in [38], and its effects consisting of harmonics amplitude reduction has been mathematically proved. are presented in The paper [39] considers the speed ripples and bars skew and presents its simulation results. In the reference [36], broken end-ring has been considered. Fig. 14 illustrates the stator current's frequency spectrum for such a case. However, the main drawback of FFT analysis is that it cannot present a localized view for the current signal. Starting current signal may be used for the fault diagnosis [4] where broken bars generate harmonics (3±4k)fr in the current spectrum (see Fig. 15). The problem of FFT with the transient signals like starting currents of the motor is solved in STFT by employing a sliding window and taking FFT from the windowed signal. However, dimensions of the window are fixed and therefore it does not have good frequency and time resolution at the same time [40]. Sometimes the current is indirectly used; for example, in [34], Park transform of the stator current has been used for fault diagnosis. Of course, this method has some drawbacks such as non-clear fault effect and susceptibility to noise; thus, it seems that the application of this method in addition to other techniques such as intelligent methods is useful. However, in this case, a set of full data is necessary. Park transform of stator current leads to iD+iQj Modulus, and harmonics arising from the broken bars fault in the line current are as 2sfs and 4sfs. The advantage of these harmonics is that they are far from the fundamental harmonic; hence, its detection is simple.

In [41], an extensive experiment for the broken rotor bar diagnosis has been performed, and comparative analysis of the zero sequence spectrum (ZSC) with conventional MCSA shows the superiority of this method. In [42], the effect of non-consecutive double bar breakage fault, its relative position on the amplitude of left sideband harmonics (LSH), and high order harmonics of the air gap field are investigated by STFT. The results showed that although the amplitude of LSH in double breakage case is smaller than single breakage, the proposed method can clearly discriminate between this fault and the healthy case.

Gabor transform is a particular case of the STFT, performed with a Gaussian window. In [43], Gabor analysis is performed on transient start-up currents for the diagnosis of the broken bar and the mixed eccentricity faults. In this method, chirp z-transform is used for the generation of very high-resolution trajectory of the fault harmonics.

Table 2. Amplitudes of the current sidebands for a motor with different rotor broken bars [4].

NBB	fs+2fr	fs-2fr
0	-58	-57
1	-54	-55
2	-53	-48
3	-48	-42
4	-46	-40

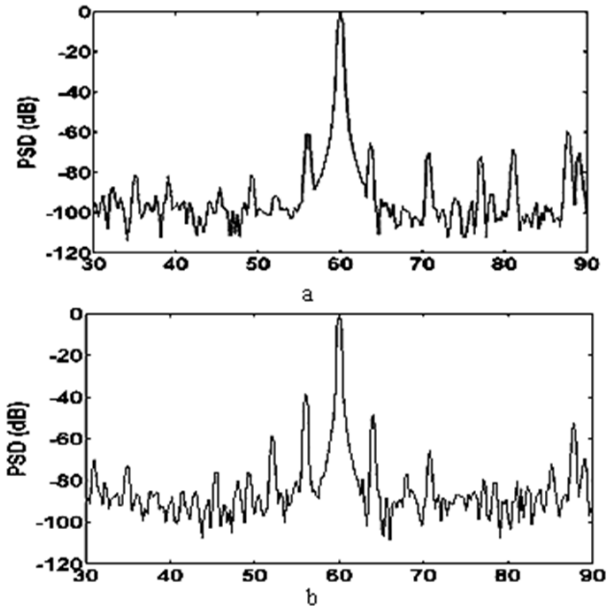

Fig. 13. Stator current stator current: (a) healthy motor, (b) motor with four rotor broken bars [4].

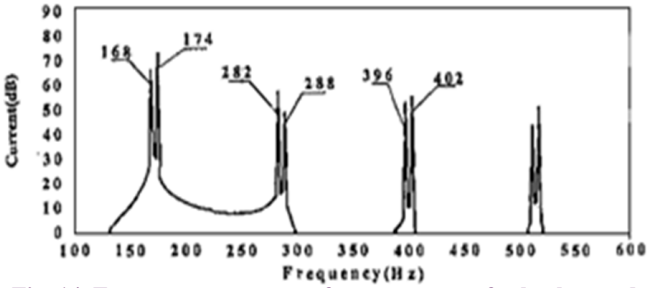

Fig. 14. Frequency spectrum of stator current for broken end-ring [36].

3- 1- 2- Impacts of Load Variation

Side-band components vary with the load torque fluctuations [44]. Fig. 16 shows time variations of stator current signal for no-load and full-load healthy and faulty induction motors with four broken bars [44]. In this figure, larger load causes a higher current and damping effect. Fig. 17 shows the impact of the load upon the high and low side-bands of the stator's current spatial vector [37]. Load fluctuation decreases the amplitude of low-band and increases the amplitude of high-band.

3- 1- 3- Impact of Broken Rotor Bars Location

Rotor bar location and its impact on the fault diagnosis have been investigated and reported in [45], and the effect of the location of the broken bar on the waveform and the frequency spectrum of the stator current and side-bands

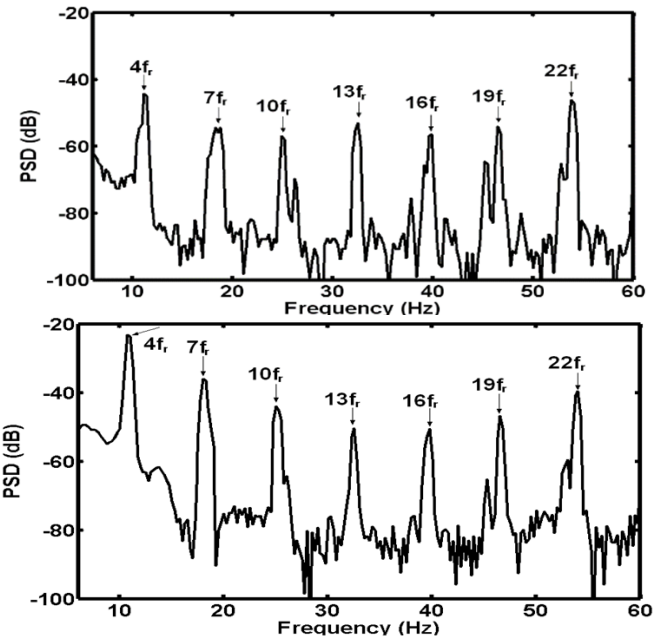

Fig. 15. Frequency spectrum of starting current: (a) healthy motor, (b) motor with 4 rotor broken bars [40].

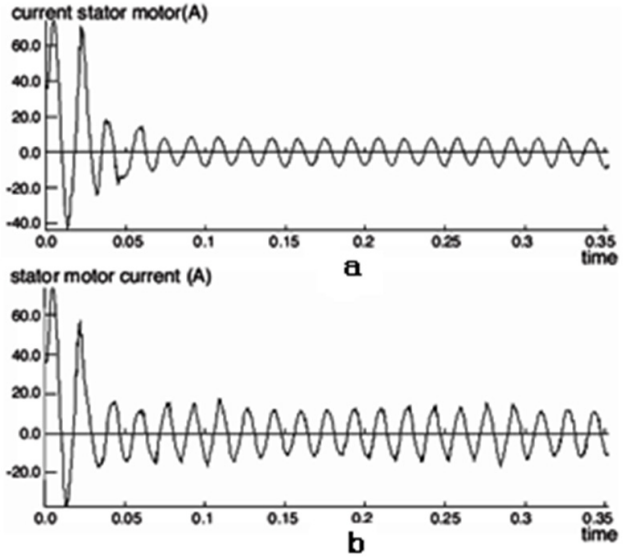

Fig. 16. Time spectrum of stator current for the motor with four rotor broken bars: (a). 50% rated load, (b). rated load [44].

components (Fig. 18) have been given. Table 3 shows that more concentrated broken bars lead to a higher amplitude of side-bands.

3- 1- 4- Impact of Drive

In the presence of drive and closed-loop circuits, the situation differs. In a PWM-driven motor, odd harmonics and third harmonic are injected to the motor. Inverter harmonic components are $f_b=(m\pm 2nks)f_s$, where m=1, 5, 7, … are odd inverter harmonics, n=1, 5, 7, … are odd harmonics due to the induced currents of the rotor and k =1, 2, 3, … is an integer number. Subsequently, odd harmonics induced in the rotor produce odd flux harmonics in the air-gap. Therefore, a new frequency pattern is introduced in the faulty motors under PWM supply [46]. In the closed-loop drive, mutual effects

of electrical and mechanical oscillations amplify each other, and the amplitude of the above-mentioned frequency spectrum increases. Fig. 19 shows an experimental stator current's spectrum for PWM-supplied the motor with the broken bars [35].

3- 2- Eccentricity Fault

Fourier transform-based processor is often used to diagnose eccentricity fault in the induction motor and different signals of IMs, including instantaneous power, phase angle, inductance profile, body vibration, and stator currents, are used in Fourier-based techniques in order to diagnose eccentricity faults. Instantaneous power spectrum has been used to diagnose two types of eccentricity simultaneously [10] in which a new method for temporal creation of eccentricity fault introduced. Identical harmonics as a result of two kinds of eccentricity in the power spectrum are produced, and in the closed-loop control, they depend on more factors. Fig. 20 shows the amplitude of the power spectrum harmonics for two different kinds of eccentricity faults [10].

Spectrum for healthy and faulty motors has been displayed in Fig. 21. The apparent power of motor can also be utilized for the fault diagnosis [7] where a criterion is expressed to determine the fault degree.

In [20], instantaneous phase power spectrum is used for the simultaneous diagnosis of two faults in an induction motor. The harmonics arising from the faults have been introduced. It is proved that due to non-overlapping between harmonics arising from individual eccentricity fault, and simultaneous occurrence of these two faults, instantaneous phase power spectrum harmonics can be used for diagnosis of this fault.

Application of Park's transform for simultaneous diagnosis of two eccentricity types is not suitable due to the cross term phenomenon in the frequency spectrum. Simultaneous occurrence of eccentricity fault is diagnosable from phase angle frequency spectrum (power factor angle) [47].

Inductance spectrum of the induction motor can be used for the simultaneous diagnosis of fault [48]. Vibration spectrum of the motor can be utilized for the fault detection. Fig. 22 shows these harmonics due to eccentricity [9]. The stator current signal has the greatest contribution to the fault type diagnosis.

3- 2- 1- Diagnosis of Eccentricity Type

Creation of some harmonics in the stator current and air gap flux density is expected due to asymmetry caused by the eccentricity fault. These harmonics consist of the harmonics around fundamental frequency and high frequencies (PSH) [1, 9, 49, 50]. Here again, most methods are based on Fourier transform. Fig. 23 shows the stator current's harmonics caused by the eccentricity fault [6]. Different eccentricity faults with their relationships are also expressed in [1]. The interaction between the harmonics arising from the dynamic and static eccentricity has been discussed in [9] in which harmonics caused by the eccentricity fault in the frequency spectrum of motor body vibration have been taken into account. Table 4 summarizes the impacts of the eccentricity fault with different degrees on the amplitude of harmonics around fundamental frequency [12]. Of course, there are low amplitude harmonics in the healthy motor due to the inherent eccentricity of the motor. PSH harmonics have been discussed in [51] and it was pointed out that the triple harmonics of poles pair must not be generated in the current spectrum. Also, a healthy motor supplied by unbalanced supply or unbalanced motor structure itself enables to generate these harmonics. Eccentricity harmonic needs some features in order to appear in the frequency spectrum; its general relationship and harmonics due to the simultaneous presence of two types of eccentricity in the frequency spectrum have been presented in [51]. Simplifying assumptions such as neglecting saturation and slot effect causes a large discrepancy between the test and theory results. Low order harmonics due to eccentricity fault are not reliable [52], because they may be caused by inherent asymmetry of the motor or unbalanced supply. Mechanical faults such as eccentricity in a medium size induction motor have been considered in [53]. Generally, PSH harmonics cannot diagnose the eccentricity type. On the other hand, bearings contaminations generate harmonics similar to those from the dynamic eccentricity fault. Misalignment fault generates frequency spectrum similar to that of the static eccentricity fault [52]. Sometimes, impulse test has been used for eccentricity fault diagnosis [8]. This is an off-line method and its frequency spectrum is an irrational spectrum and cannot be considered as fault degree criterion. Fig. 24 shows the impulse test results for a faulty motor [8].

In [54], the spectrum of the terminal voltage of the machine at switch-off is used to detect all types of eccentricity faults. Because of transient nature of this signal, STFT is used for the spectrum calculations. At switch-off, UMP will not exist due to the cessation of stator rotating magnetic field. Therefore, this method is independent of UMP. In addition, unlike current based methods in which some of the fault components may disappear for a certain pole pair and rotor slot combination, this method is applicable to any machine.

3- 2- 2- Impacts of Load Variation

Both the eccentricity fault and the load have a similar impact on the spectrum of the current [6]. In this case, side-band frequencies and their amplitudes are used for the fault diagnosis. Table 4 summarizes the amplitude of harmonics around the fundamental frequency and also PSH harmonics in healthy and static eccentric motor [6]. A higher load decreases the amplitude of the proposed harmonics. Fig. 25 shows the impacts of the load fluctuations and eccentricity degree upon the amplitude of harmonics around the fundamental frequency and PSH harmonics [6].

It indicates that increasing the load and dynamic eccentricity degree increases the amplitude of the harmonics around PSH. It means that the highest amplitude of harmonics is at the rated load and maximum eccentricity degree. Only the rate of the impact of the load and the dynamic eccentricity fault upon the amplitude of harmonics differs. The rate of increase of the harmonic amplitude around PSH by rising fault degree at a fixed load is larger than that of increasing the load at the fixed fault degree. Finally, for diagnosis of the eccentricity fault, harmonics around fundamental frequency can be used and for simultaneous diagnosis of the eccentricity fault and its type, harmonics around PSH can be utilized.

3- 2- 3- Impact of Drive

In a controlled motor, high-order harmonics have a higher amplitude and are the dominant harmonics in the motor. Therefore, in this case, the frequency pattern can be used as the eccentricity fault index by more investigation of the impact of the motor's operating conditions upon this

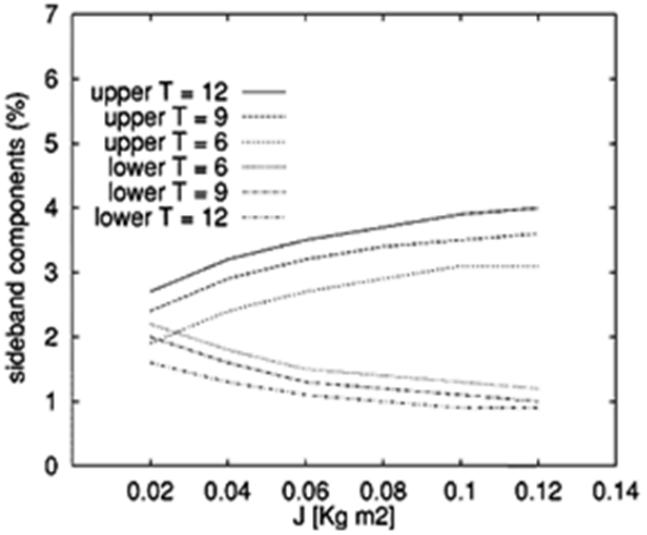

Fig. 17. Impact of load upon high and low side-bands of stator current spatial vector [40].

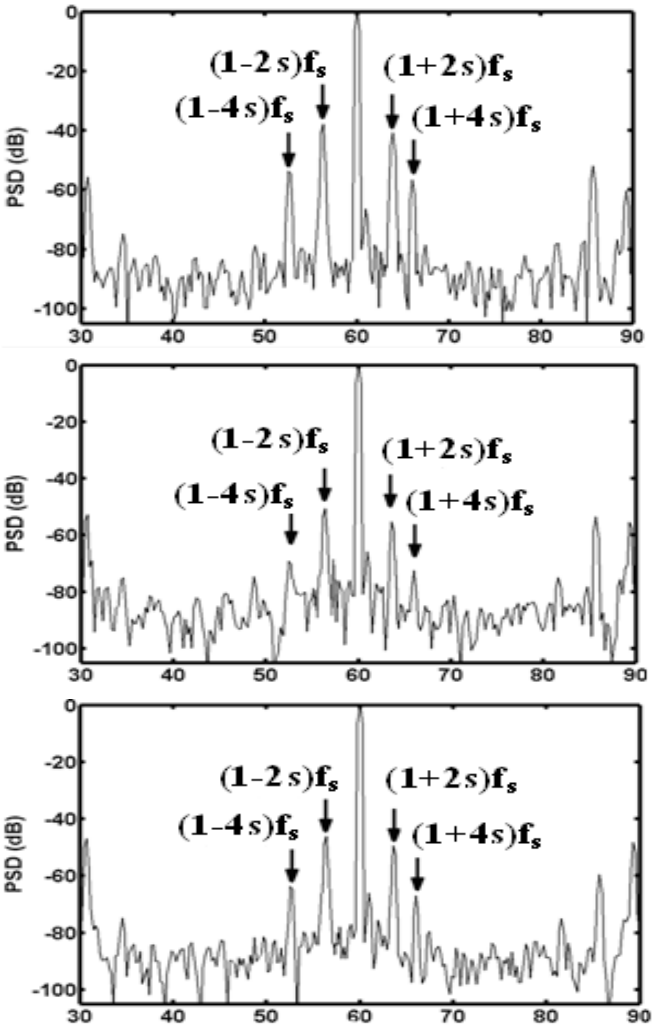

Fig. 18. Impact of bars location on the amplitude of sidebands; (a) three broken bars in one pole and one broken bar in adjacent pole, (b) two broken bars in one pole and two broken bars in the adjacent pole, (c) one bar under each pole [45].

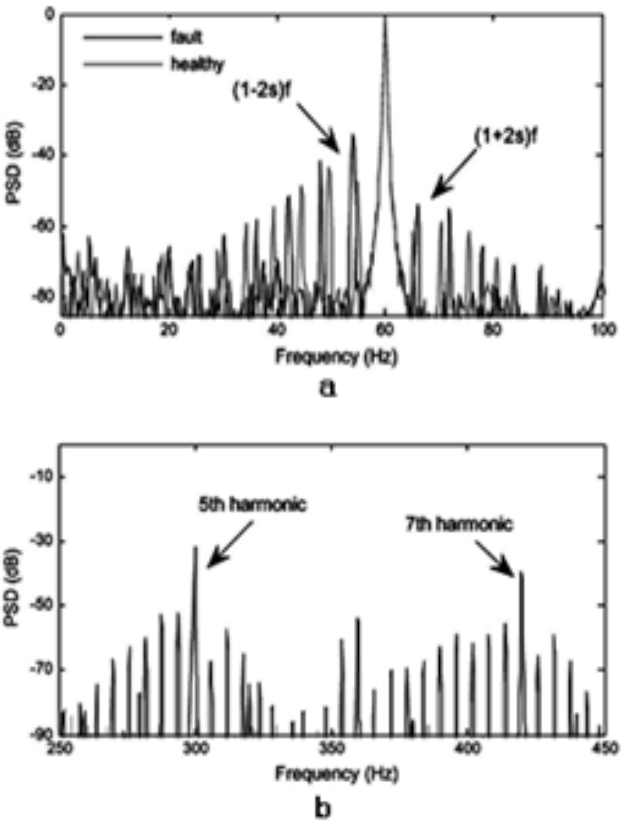

Fig. 19. Experimental stator current spectrum in PWM supplied motor with the broken bars [35]

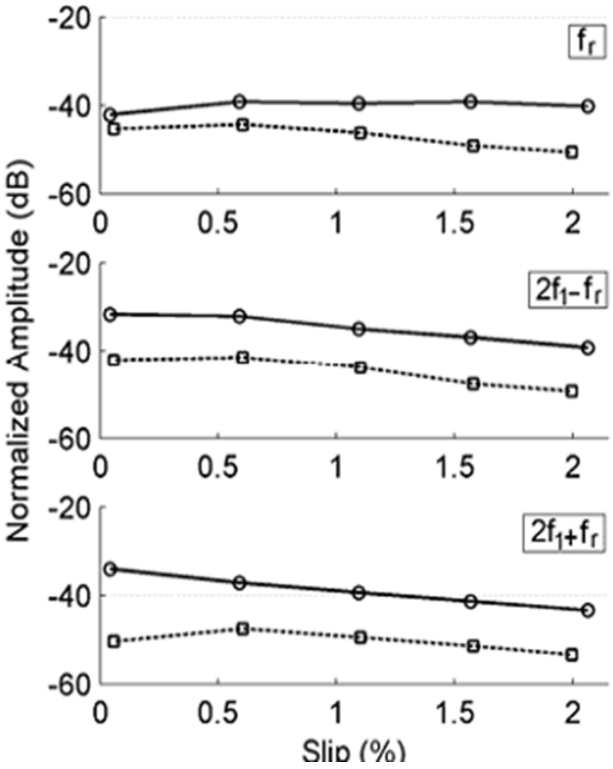

Fig. 20. Amplitude of power spectrum harmonics for two different eccentricity faults [10].

index. Of course, the same results cannot be expected for the different drives. The sum of the amplitudes of the first sidebands around the fundamental harmonic of the motor is studied as the eccentricity fault diagnosis index in [55]. This index is somehow robust against load fluctuations in both the direct supply and controlled cases. In spite of this, the amplitude of this index does not show a fixed trend against variation of the parameters of DTC controlled motor. PI controllers in FOC drive operate as a low-pass filter, and the amplitudes of sidebands of the fundamental frequency are affected by the bandwidth of controllers. In FOC drive, PSH spectrum will be eliminated, because it is located within a high frequency range. Almost there is no such a problem in DTC drive without the speed loop. Therefore, the use of sidebands of the fundamental harmonic index will operate better in DTC compared with that of FOC. In [10], the active power of motor has been investigated for the mixed eccentricity fault diagnosis in direct-supply, open-loop scalar controlled (v/f) and DTC closed-loop controlled cases. Fig. 26 shows a typical power spectrum of a motor under eccentricity for three drives. In the direct-supply case, all harmonics obtained from equations are visible. In v/f open-loop controlled motor, two low harmonics are present but the amplitude of the high harmonic is lower than that of the noise level . No reason has been so far given for such a reduction. There are all three harmonics in the DTC closed-loop drive. According to the experimental results, the behavior of v/f drive shows opposite to that of DTC with different loads and speeds. v/f drive increases the harmonics amplitude compared with the line-start case, but DTC drive decreases the amplitude of these harmonics. DTC drive has no considerable effect on the amplitude of the index over low loads and also speed variations. However, in v/f case, the amplitude of the index varies for some loads.

3- 3- Bearing Fault

Fourier based methods have more contribution in bearing fault diagnosis. Some methods have been introduced for bearing fault diagnosis based on the harmonics and their impacts on the frequency spectrum of the current [56, 57]. These methods do not require the bearing parameters of the motor and are based on the noise deletion. Different kinds of bearing faults and load influences on the harmonics arising from fault have been investigated in [14]. It has been shown that the amplitude of harmonics decreases by increasing the load due to the damping effect of the load. Fig. 27 shows the frequency spectrum of a healthy motor and a motor under a bearing fault [14]. For the same fault degree, harmonic components due to the fault on the external flake of bearing are larger than that of the internal flake. The fault can be better diagnosed in the no-load case because of load harmonics deletion. Both axial and radial movement of the rotor due to the fault can be considered, and a model is introduced based on the load torque fluctuations and also the variation of the air gap length [13]. Since frequency components mainly depend on the load and fault type, it has been suggested to use a vibration frequency spectrum in addition to the current frequency spectrum for fault diagnosis. Here FFT with Hilbert transform is utilized to diagnose the fault. In [46], bearing fault in a PWM-driven motor has been proposed and Fig. 28 exhibits frequency spectrum of body vibration of the faulty motor in which external flake bearing fault occurs. This fault increases particular harmonics amplitudes that are introduced in Fig. 28. Fourier series-based methods can be useful in specific cases

Table 3. Amplitude of current sidebands versus rotor broken bars positions [45]

Location of broken bars	(1-2s) fs	(1+2s) fs	(1-4s) fs	(1+4s) fs
Four broken bars on one pole	-38	-40	-54	-56
Three broken bars on one pole and one broken bar on the adjacent pole	-40	-42	-57	-60
Three broken bars on one pole and one broken bar on the opposite pole	-41	-44	-59	-60
Two broken bars on one pole and two broken bars on the adjacent pole	-43	-45	-60	-63
Two broken bars on one pole and two broken bars on two adjacent poles	-45	-47	-63	-66
Two broken bars on one pole and one broken bar on adjacent and opposite pole	-46	-50	-64	-67
Two broken bars on one pole and two broken bars on opposite pole	-48	-52	-67	-69
One broken bar on each pole	-51	-55	-70	-73
One broken only on one pole	-54	-59	-73	-77
Healthy motor	-60	-63	-76	-90

and goals. First, the employed signals must be a steady-state and stable signal in order to minimize the error due to the transformation. However, some have used STFT for transient signals and their disadvantages have been described above. Secondly, a fundamental component of the current makes it difficult to follow the fault diagnosis process in the no-load case; thus, a load is required for fault diagnosis using this method [58]. Therefore, the fundamental component of the current must be deleted and this deletion will cause some changes in other harmonics due to the fault. Also, transient signals, such as starting current of the machine, have useful information for the fault diagnosis. Advantages of the transient signals are as it follows [58, 59]:

1. frequency components of transient mode due to the fault have a higher amplitude compared with that of the steady-state mode;
2. transient spectrum has a series of additional data.

In [60], STFT is used for the fault detection of bearing failure due to circulating currents caused by motor variable frequency drives. The reason for using t-f methods in the analysis of vibration signal is that continues tracking of fault components regardless of the machine operation conditions is possible as STFT can visualize the evolution of frequency components over time. Also, this method shows discrimination for different kinds of bearings.

4- Conclusions

In this survey, different methods and processors used for the diagnosis of three internal faults of induction motors were investigated briefly. To this end, four types of processors and their advantages and drawbacks were studied. It is clear that a

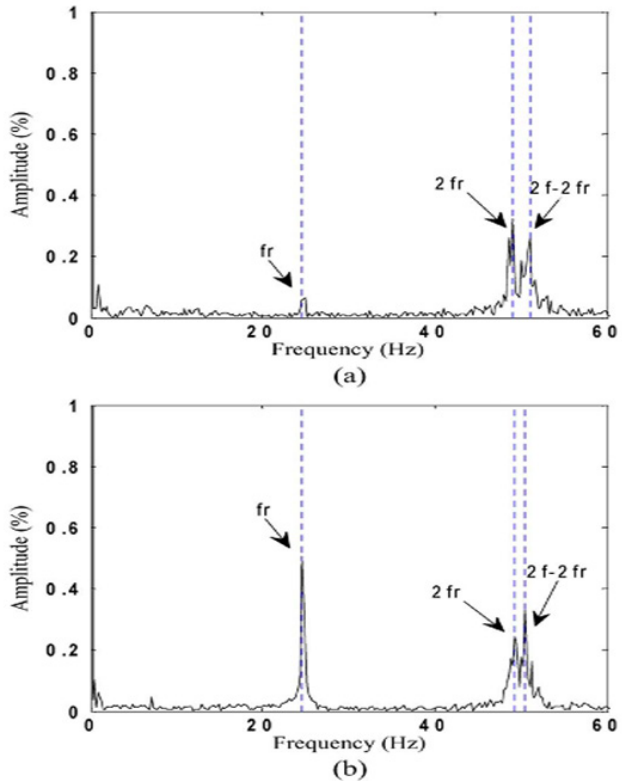

Fig. 21. Power spectrum harmonics, (a) healthy motor, (b) motor with 33% static eccentricity [7].

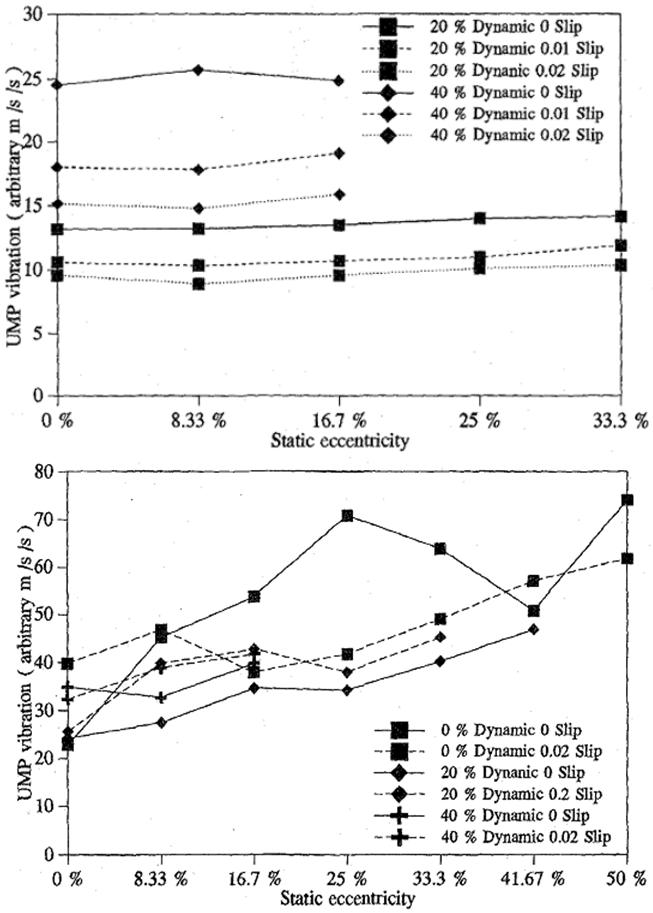

Fig. 22. Vibration spectrum harmonics due to eccentricity: (a) UMP vibration ;(b) twice-supply-frequency vibration [9].

Table 4. Amplitude of harmonics around fundamental frequency and also PSH harmonics in healthy and static eccentric motor [6]

	Healthy motor	Motor with 41% SE
% of Rated load	PSH	PSH
0	-52	-50
33	-44	-41
66	-38	-34
100	-33	-30

	Healthy motor				Motor with 41% SE			
% of Rated load	f_s-f_r	f_s+f_r	f_s+2f_r	f_s+3f_r	f_s-f_r	f_s+f_r	f_s+2f_r	f_s+3f_r
0	-78	-79	-64	-90	-54	-55	-59	-78
33	-70	-76	-66	-87	-60	-57	-61	-80
66	-76	-77	-70	-85	-68	-65	-62	-83
100	-80	-78	-85	-86	-70	-69	-76	-85

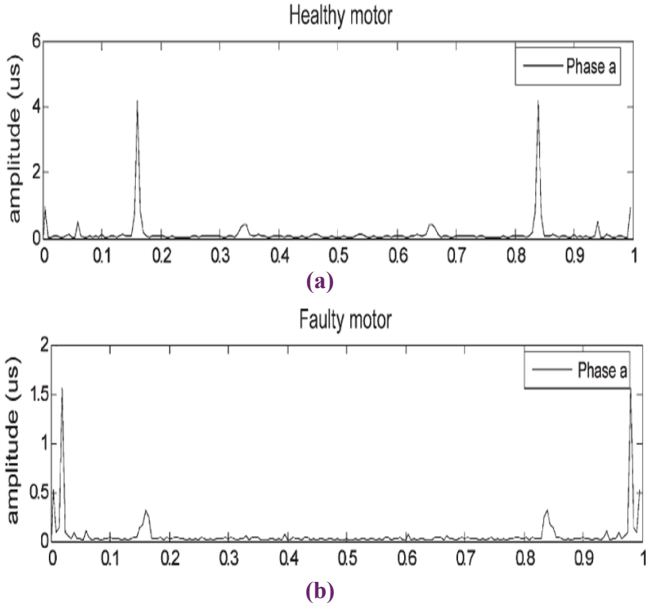

Fig. 24. Impulse test results, (a) Healthy motor, (b) faulty motor [8]

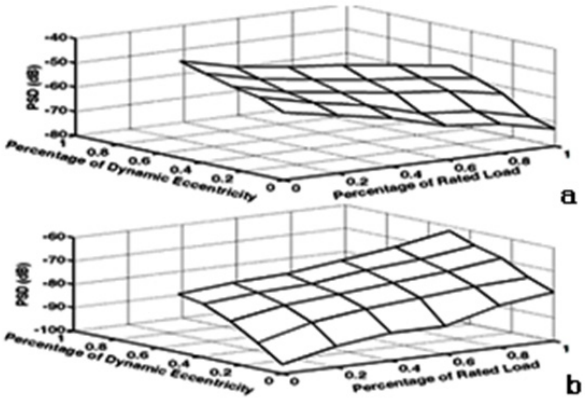

Fig. 25. Load fluctuations impacts and eccentricity degree upon the amplitude of harmonics around the fundamental frequency and PSH harmonics [6].

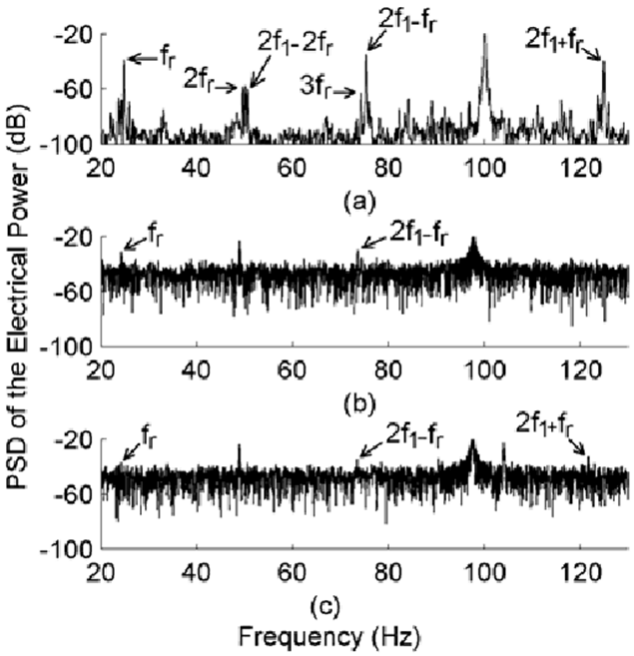

Fig. 26. Frequency spectrum of instantaneous power: (a) Direct supply, (b) DTC and (c) CVF [10].

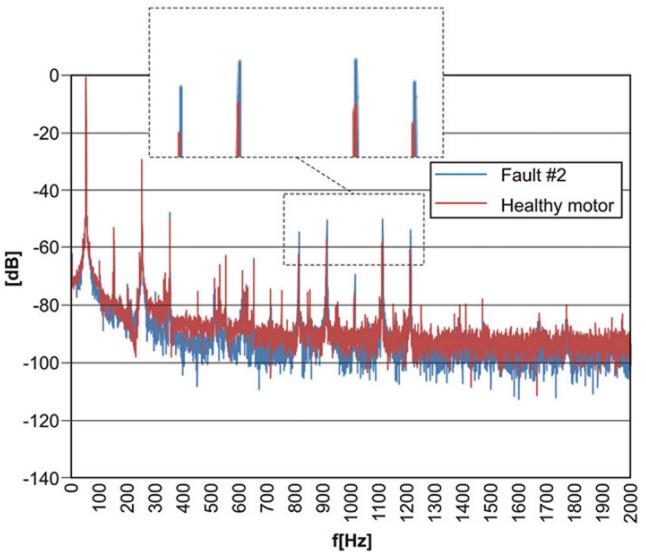

Fig. 27. Frequency spectrum of stator current for healthy motor and motor under bearing fault at full load. [14].

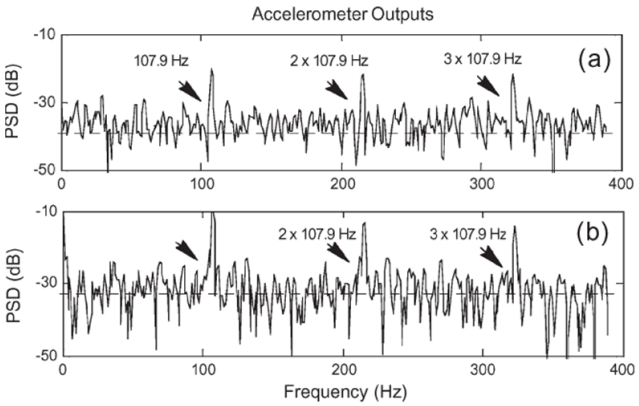

Fig. 28. Frequency spectrum of body vibration with fault in external flake of bearing [46].

single method and a common processor cannot be specified for all faults. Fourier processor as the most applicable processor for different faults has weak and strong points. Its most important weakness is in the processing of transient signals. To overcome this problem, applying a wavelet processor was suggested. This provides more detailed time and frequency view of the signal. Wavelet pockets with the simultaneous high precision of time and frequency are commonly used. These processors are often used for the broken bars fault but there are no appropriate studies on the number of broken bars and their locations. Other drawbacks of this method are that it is time-consuming and suffers from complicated technique. In recent years, Hilbert-based techniques with a high-frequency precision methods such as MUSIC have been proposed. A common point that must be taken into account in an appropriate fault diagnosis method in industry beside on-line case is that the method must be quick and at the same time must have a high level of accuracy.

References

[1] J. Faiz, B.M. Ebrahimi, M.B.B. Sharifian, Different Faults and Their Diagnosis Techniques in Three-Phase Squirrel-Cage Induction Motors—A Review, Electromagnetics, 26 (2006) 543-569.

[2] S. Nandi, H.A. Toliyat, X. Li, Condition Monitoring and Fault Diagnosis of Electrical Motors—A Review, IEEE Transactions on Energy Conversion, 20(4) (2005) 719-729.

[3] X. Ying, Characteristic Performance Analysis of Squirrel Cage Induction Motor With Broken Bars, IEEE Transactions on Magnetics, 45 (2009) 759-766.

[4] J. Faiz, B.-M. Ebrahimi, A New Pattern for Detecting Broken Rotor Bars in Induction Motors During Start-Up, IEEE Transactions on Magnetics, 44 (2008) 4673-4683.

[5] J. Faiz, B.M. Ebrahimi, Determination of Number of Broken Rotor Bars and Static Eccentricity Degree in Induction Motor under Mixed Fault, Electromagnetics, 28 (2008) 433-449.

[6] J. Faiz, B.M. Ebrahimi, B. Akin, H.A. Toliyat, Comprehensive Eccentricity Fault Diagnosis in Induction Motors Using Finite Element Method, IEEE Transactions on Magnetics, 45 (2009) 1764-1767.

[7] M. Drif, A.J.M. Cardoso, Airgap-Eccentricity Fault Diagnosis, in Three-Phase Induction Motors, by the Complex Apparent Power Signature Analysis, IEEE Transactions on Industrial Electronics, 55 (2008) 1404-1410.

[8] X. Huang, T.G. Habetler, R.G. Harley, E.J. Wiedenbrug, Using a Surge Tester to Detect Rotor Eccentricity Faults in Induction Motors, IEEE Transactions on Industry Applications, 43 (2007) 1183-1190.

[9] [9] D.G. Dorrell, W.T. Thomson, S. Roach, Analysis of airgap flux, current, and vibration signals as a function of the combination of static and dynamic airgap eccentricity in 3-phase induction motors, IEEE Transactions on Industry Applications, 33 (1997) 24-34.

[10] J. Faiz, M. Ojaghi, Instantaneous-Power Harmonics as Indexes for Mixed Eccentricity Fault in Mains-Fed and Open/Closed-Loop Drive-Connected Squirrel-Cage Induction Motors, IEEE Transactions on Industrial Electronics, 56 (2009) 4718-4726.

[11] S. Nandi, R.M. Bharadwaj, H.A. Toliyat, Performance analysis of a three-phase induction motor under mixed eccentricity condition, IEEE Transactions on Energy Conversion, 17 (2002) 392-399.

[12] J. Faiz, B.M. Ebrahimi, B. Akin, H.A. Toliyat, Finite-Element Transient Analysis of Induction Motors Under Mixed Eccentricity Fault, IEEE Transactions on Magnetics, 44 (2008) 66-74.

[13] M. Blodt, P. Granjon, B. Raison, G. Rostaing, Models for Bearing Damage Detection in Induction Motors Using Stator Current Monitoring, IEEE Transactions on Industrial Electronics, 55 (2008) 1813-1822.

[14] L. Frosini, E. Bassi, Stator Current and Motor Efficiency as Indicators for Different Types of Bearing Faults in Induction Motors, IEEE Transactions on Industrial Electronics, 57 (2010) 244-251.

[15] I.Y. Önel, M.E.H. Benbouzid, Induction Motor Bearing Failure Detection and Diagnosis: Park and Concordia Transform Approaches Comparative Study, IEEE/ASME Transactions on Mechatronics, 13 (2008) 257-262.

[16] M.J. Devaney, L. Eren, Detecting motor bearing faults, IEEE Instrumentation and Measurement Magazine, 7 (2004) 30-50.

[17] L. Eren, M.J. Devaney, Bearing Damage Detection via Wavelet Packet Decomposition of the Stator Current, IEEE Transactions on Instrumentation and Measurement, 53 (2004) 431-436.

[18] B. Mirafzal, N.A.O. Demerdash, On innovative methods of induction motor interturn and broken-bar fault diagnostics, IEEE Transactions on Industry Applications, 42 (2006) 405-414.

[19] J. Faiz, I. Tabatabaei, Extension of winding function theory for nonuniform air gap in electric machinery, IEEE Transactions on Magnetics, 38 (2002) 3654-3657.

[20] Z. Liu, X. Yin, Z. Zhang, D. Chen, W. Chen, Online Rotor Mixed Fault Diagnosis Way Based on Spectrum Analysis of Instantaneous Power in Squirrel Cage Induction Motors, IEEE Transactions on Energy Conversion, 19 (2004) 485-490.

[21] M.S. Ballal, Z.J. Khan, H.M. Suryawanshi, R.L. Sonolikar, Adaptive Neural Fuzzy Inference System for the Detection of Inter-Turn Insulation and Bearing Wear Faults in Induction Motor, IEEE Transactions on Industrial Electronics, 54 (2007) 250-258.

[22] S. Shin, J. Kim, S.B. Lee, C. Lim, E.J. Wiedenbrug, Evaluation of the Influence of Rotor Magnetic Anisotropy on Condition Monitoring of Two-Pole Induction Motors, IEEE Transactions on Industry Applications, 51 (2015) 2896-2904.

[23] A. Sadeghian, Z. Ye, B. Wu, Online Detection of Broken Rotor Bars in Induction Motors by Wavelet Packet Decomposition and Artificial Neural Networks, IEEE Transactions on Instrumentation and Measurement, 58 (2009) 2253-2263.

[24] J.F. Bangura, R.J. Povinelli, N.A.O. Demerdash, R.H. Brown, Diagnostics of eccentricities and bar/end-ring connector breakages in polyphase induction motors through a combination of time-series data mining and time-stepping coupled fe~state-space techniques, IEEE Transactions on Industry Applications, 39 (2003) 1005-1013.

[25] S.H. Kia, H. Henao, G.-A. Capolino, Diagnosis of Broken-Bar Fault in Induction Machines Using Discrete Wavelet Transform Without Slip Estimation, IEEE Transactions on Industry Applications, 45 (2009) 1395-1404.

[26] M.E.H. Benbouzid, G.B. Kliman, What stator current processing-based technique to use for induction motor rotor faults diagnosis?, IEEE Transactions on Energy Conversion, 18 (2003) 238-244.

[27] P.J. Rodriguez, A. Belahcen, A. Arkkio, Signatures of electrical faults in the force distribution and vibration pattern of induction motors, IEE Proceedings - Electric Power Applications, 153 (2006) 523.

[28] C.-C. Yeh, G.Y. Sizov, A. Sayed-Ahmed, N.A.O. Demerdash, R.J. Povinelli, E.E. Yaz, D.M. Ionel, A Reconfigurable Motor for Experimental Emulation of Stator Winding Interturn and Broken Bar Faults in Polyphase Induction Machines, IEEE Transactions on Energy Conversion, 23 (2008) 1005-1014.

[29] B. Mirafzal, N.A.O. Demerdash, Effects of Load Magnitude on Diagnosing Broken Bar Faults in Induction Motors Using the Pendulous Oscillation of the Rotor Magnetic Field Orientation, IEEE Transactions on Industry Applications, 41 (2005) 771-783.

[30] G. Didier, E. Ternisien, O. Caspary, H. Razik, Fault detection of broken rotor bars in induction motor using a global fault index, IEEE Transactions on Industry Applications, 42 (2006) 79-88.

[31] J. Milimonfared, H.M. Kelk, S. Nandi, A.D. Minassians, H.A. Toliyat, A novel approach for broken-rotor-bar detection in cage induction motors, IEEE Transactions on Industry Applications, 35 (1999) 1000-1006.

[32] A.M. da Silva, R.J. Povinelli, N.A.O. Demerdash, Induction Machine Broken Bar and Stator Short-Circuit Fault Diagnostics Based on Three-Phase Stator Current Envelopes, IEEE Transactions on Industrial Electronics, 55 (2008) 1310-1318.

[33] C.-E. Kim, Y.-B. Jung, S.-B. Yoon, D.-H. Im, The fault diagnosis of rotor bars in squirrel cage induction motors by time-stepping finite element method, IEEE Transactions on Magnetics, 33 (1997) 2131-2134.

[34] M. Haji, H.A. Toliyat, Pattern recognition-a technique for induction machines rotor broken bar detection, IEEE Transactions on Energy Conversion, 16 (2001) 312-317.

[35] R. Puche-Panadero, M. Pineda-Sanchez, M. Riera-Guasp, J. Roger-Folch, E. Hurtado-Perez, J. Perez-Cruz, Improved Resolution of the MCSA Method Via Hilbert Transform, Enabling the Diagnosis of Rotor Asymmetries at Very Low Slip, IEEE Transactions on Energy Conversion, 24 (2009) 52-59.

[36] J.F. Bangura, N.A. Demerdash, Diagnosis and characterization of effects of broken bars and connectors in squirrel-cage induction motors by a time-stepping coupled finite element-state space modeling approach, IEEE Transactions on Energy Conversion, 14 (1999) 1167-1176.

[37] A. Bellini, F. Filippetti, G. Franceschini, C. Tassoni, G.B. Kliman, Quantitative evaluation of induction motor broken bars by means of electrical signature analysis,

IEEE Transactions on Industry Applications, 37 (2001) 1248-1255.

[38] R.F. Walliser, C.F. Landy, Determination of interbar current effects in the detection of broken rotor bars in squirrel cage induction motors, IEEE Transactions on Energy Conversion, 9 (1994) 152-158.

[39] J.F. Watson, D.G. Dorrell, The use of finite element methods to improve techniques for the early detection of faults in 3-phase induction motors, IEEE Transactions on Energy Conversion, 14 (1999) 655-660.

[40] P.V. Goode, M.-y. Chow, Using a neural/fuzzy system to extract heuristic knowledge of incipient faults in induction motors. Part I-Methodology, IEEE Transactions on Industrial Electronics, 42 (1995) 131-138.

[41] K. Gyftakis, J. Antonino-Daviu, R. Garcia-Hernandez, M. McCulloch, D. Howey, A. Cardoso, Comparative Experimental Investigation of the Broken Bar Fault Detectability in Induction Motors, IEEE Transactions on Industry Applications, 10 (2015) 1-1.

[42] M. Riera-Guasp, J. Pons-Llinares, F. Vedreño-Santos, J.A. Antonino-Daviu, M. Fernández Cabanas, Evaluation of the amplitudes of high-order fault related components in double bar faults, SDEMPED 2011 - 8th IEEE Symposium on Diagnostics for Electrical Machines, Power Electronics and Drives, (2011) 307-315.

[43] M. Riera-Guasp, M. Pineda-Sanchez, J. Perez-Cruz, R. Puche-Panadero, J. Roger-Folch, J.A. Antonino-Daviu, Diagnosis of induction motor faults via gabor analysis of the current in transient regime, IEEE Transactions on Instrumentation and Measurement, 61 (2012) 1583-1596.

[44] J. Faiz, B.M. Ebrahimi, M.B.B. Sharifian, TIME STEPPING FINITE ELEMENT ANALYSIS OF BROKEN BARS FAULT IN A THREE-PHASE SQUIRREL-CAGE INDUCTION MOTOR, Progress In Electromagnetics Research, 68 (2007) 53-70.

[45] J. Faiz, B.M. Ebrahimi, Locating rotor broken bars in induction motors using finite element method, Energy Conversion and Management, 50 (2009) 125-131.

[46] B. Akin, U. Orguner, H.A. Toliyat, M. Rayner, Low Order PWM Inverter Harmonics Contributions to the Inverter-Fed Induction Machine Fault Diagnosis, IEEE Transactions on Industrial Electronics, 55 (2008) 610-619.

[47] M.h. Drif, A.J.M. Cardoso, The Use of Instantaneous Phase-Angle Signature Analysis for Airgap Eccentricity Diagnosis in Three-Phase Induction Motors, in: 2007 International Conference on Power Engineering, Energy and Electrical Drives, IEEE, 2007, pp. 100-105.

[48] J. Faiz, I.T. Ardekanei, H.A. Toliyat, An evaluation of inductances of a squirrel-cage induction motor under mixed eccentric conditions, IEEE Transactions on Energy Conversion, 18 (2003) 252-258.

[49] W.T. Thomson, A. Barbour, On-line current monitoring and application of a finite element method to predict the level of static airgap eccentricity in three-phase induction motors, IEEE Transactions on Energy Conversion, 13 (1998) 347-357.

[50] J.F. Bangura, N.A. Demerdash, Effects of broken bars/end-ring connectors and airgap eccentricities on ohmic and core losses of induction motors in ASDs using a coupled finite element-state space method, IEEE Transactions on Energy Conversion, 15 (2000) 40-47.

[51] S. Nandi, S. Ahmed, H.A. Toliyat, Detection of rotor slot and other eccentricity related harmonics in a three phase induction motor with different rotor cages, IEEE Transactions on Energy Conversion, 16 (2001) 253-260.

[52] X. Li, Q. Wu, S. Nandi, Performance Analysis of a Three-Phase Induction Machine With Inclined Static Eccentricity, IEEE Transactions on Industry Applications, 43 (2007) 531-541.

[53] A.M. Knight, S.P. Bertani, Mechanical Fault Detection in a Medium-Sized Induction Motor Using Stator Current Monitoring, IEEE Transactions on Energy Conversion, 20 (2005) 753-760.

[54] S. Nandi, T.C. Ilamparithi, S.B. Lee, D. Hyun, Detection of eccentricity faults in induction machines based on nameplate parameters, IEEE Transactions on Industrial Electronics, 58 (2011) 1673-1683.

[55] M. Ojaghi, Eccentricity fault diagnosis in three-phase induction motors under mains voltage and DTC drive supply modes, Ph. D. thesis, School of Electrical and Computer Engineering, Univ. Tehran, Tehran, Iran, (2009).

[56] W. Zhou, B. Lu, T.G. Habetler, R.G. Harley, Incipient Bearing Fault Detection via Motor Stator Current Noise Cancellation Using Wiener Filter, IEEE Transactions on Industry Applications, 45 (2009) 1309-1317.

[57] Y. Liu, L. Guo, Q. Wang, G. An, M. Guo, H. Lian, Application to induction motor faults diagnosis of the amplitude recovery method combined with FFT, Mechanical Systems and Signal Processing, 24 (2010) 2961-2971.

[58] M. Riera-Guasp, J.A. Antonino-Daviu, M. Pineda-Sanchez, R. Puche-Panadero, J. Perez-Cruz, A General Approach for the Transient Detection of Slip-Dependent Fault Components Based on the Discrete Wavelet Transform, IEEE Transactions on Industrial Electronics, 55 (2008) 4167-4180.

[59] M. Timusk, M. Lipsett, C.K. Mechefske, Fault detection using transient machine signals, Mechanical Systems and Signal Processing, 22 (2008) 1724-1749.

[60] A. Prudhom, J. Antonino-Daviu, H. Razik, V. Climente-Alarcon, Time-frequency vibration analysis for the detection of motor damages caused by bearing currents, Mechanical Systems and Signal Processing, (2015) 1-16.

Please cite this article using:

J. Faiz, A. M. Takbash, E. Mazaheri-Tehrani, A Review of Application of Signal Processing Techniques for Fault Diagnosis of Induction Motors – Part I, *AUT J. Elec. Eng.,* 49(2)(2017)109-122.

DOI: 10.22060/eej.2017.13219.5142